

$B_n(BO)_n^{2-}$, $CB_{n-1}(BO)_n^-$, and $C_2B_{n-2}(BO)_n$ ($n=5-12$): Cage-like boron oxide clusters analogous to $closoboranes B_nH_n^{2-}$, $CB_{n-1}H_n^-$, and $C_2B_{n-2}H_n$

MIAO ChangQing & LI SiDian*

Institute of Materials Sciences and Department of Chemistry, Xinzhou Teachers University, Xinzhou 034000, China

Received June 13, 2010; accepted August 27, 2010

A density functional theory (DFT) investigation has been performed in this work on the cage-like boron-rich boron oxide clusters $B_n(BO)_n^{2-}$, $CB_{n-1}(BO)_n^-$, and $C_2B_{n-2}(BO)_n$ ($n=5-12$) which are boronyl analogues of the *closoboranes* $B_nH_n^{2-}$, monocarbaboranes $CB_{n-1}H_n^-$, and dicarbaboranes $C_2B_{n-2}H_n$. These boron oxide clusters possess similar geometrical and electronic structures with the corresponding boranes and carboranes and prove to be three-dimensional (3D) aromatic compounds, consistent with the previously proposed BO/H isolobal analogy. Neutral $C_2B_{n-2}(BO)_n$ species possess considerably high ionization potentials in the range 12.0–12.7 eV and $CB_{n-1}H_n^-$ monoanions have the vertical electron detachment energies in the range 6.6–9.4 eV at the DFT level. BO terminals singly bonded to the skeletal vertexes through a B atom possess the characteristic stretching vibrational frequencies at about 2000 cm^{-1} , clearly indicating the existence of $\text{B}\equiv\text{O}$ triple bonds in these clusters. Experimental syntheses and characterizations of these interesting clusters may expand the structural concepts of boron oxides and bring important applications for boron oxide clusters as molecular devices in chemistry and new materials in boron neutron capture therapy.

boron oxide clusters, boronyl group, density functional theory, geometrical structures, electronic structures, aromaticities

1 Introduction

As prototypical electron-deficient systems, *closoboranes* ($B_nH_n^{2-}$), monocarbaboranes ($CB_{n-1}H_n^-$), and dicarbaboranes ($C_2B_{n-2}H_n$) ($n=5-12$) possess cage-like structures with n vertexes and $n+1$ skeletal electron pairs and feature three-dimensional (3D) aromaticities, high resonance stabilities, and benzene-like reactivities (electrophilic substitutions) [1–5]. The highly symmetrical $D_{5d} C_2B_{10}H_{12}$ which has been described as a “superatom” has found wide applications in chemistry and in neutron capture therapies. Boron oxide B_xO_y clusters, another important class of boron compounds, on the other hand, feature predominantly BO_3 planar trian-

gular units in 3D or 2D networks [1, 6]. No direct structural link was discovered between boron oxides and boron hydrides before 2007 when the concept of boronyl (BO) in monocyclic carbon boronyls ($C_n(\text{BO})_n$, $n=2-7$) was proposed by our group at the density functional theory (DFT) level [7]. This concept was later extended to transition metal sandwich complexes [8], the boronyl-substituted ethylenes and acetylenes [9], tetrahedral $\text{B}(\text{BO})_4^-$ [10], and the closely related BS-containing compounds [11, 12]. In three joint photoelectron spectroscopy (PES) and *ab initio* studies, Zhai, Li, and Wang revealed, for the first time, the σ -radical nature of the triply bonded boronyl group ($\text{B}\equiv\text{O}$) [13] and the BO/H isolobal relationship in linear $\text{B}(\text{BO})_2$ and triangular $\text{B}(\text{BO})_3^-$ [14], and linear $[\text{O}=\text{B}-\text{B}=\text{B}=\text{B}=\text{O}]^{0/-2-}$ [15]. The boronyl pattern established in these investigations builds a clear structural link between the boron-rich boron

*Corresponding author (email: lisidian@yahoo.com)

oxide clusters formulated as $B_m(BO)_n$ and the corresponding boron hydrides B_mH_n . Small boron-rich B_xO_y microclusters ($x=1-10$; $y=1-3$) have also been systematically investigated at the DFT levels, and the results suggested the existence of BO groups in a wide range of boron oxide clusters [16-18]. The first stable $[(Cy_3P)_2BrPt(BO)]$ crystal with a triply bonded $B \equiv O$ ligand was synthesized and characterized in 2010 by Braunschweig and co-workers, opening the era of boronyl chemistry [19]. In this work, we perform a systematic DFT investigation on the cage-like $B_n(BO)_n^{2-}$, $CB_{n-1}(BO)_n^-$, and $C_2B_{n-2}(BO)_n$ ($n=5-12$) clusters which are the boronyl analogues of the *closo*-species $B_nH_n^{2-}$, $CB_{n-1}H_n^-$, and $C_2B_{n-2}H_n$. These novel boron oxide clusters, which are larger in size than any boron oxide clusters reported before [6-18], prove to be 3D aromatic and possess similar geometrical and electronic structures with their parent boranes or carboranes, with the 6, 10, and 12-vertex cage-like species being the most 3D aromatic species (except the $B_6(BO)_6^{2-}$ and $B_{12}(BO)_{12}^{2-}$ dianions). Experimental syntheses and characterization of these polyhedral boron oxide clusters are expected to expand our knowledge of the structural concepts for boron oxides and bring important applications for boron oxide clusters as molecular devices in chemistry and new materials in boron neutron capture therapy [1-5].

2 Theoretical methods

Structural optimizations, frequency analyses, and natural bond orbital (NBO) analyses were performed using the hybrid B3LYP/6-311+G(3df) method [20, 21]. To check the 3D aromaticities of the optimized cage structures, the magnetic susceptibilities (χ) and the nucleus independent chemical shifts (NICS) at the geometrical centers of the cages [22] were calculated using the continuous set of gauge transformations (CSGT) method [23, 24]. To facilitate future ex-

perimental characterizations of these clusters, the ionization potentials (IPs) of $C_2B_{n-2}(BO)_n$ neutrals calculated as the energy differences between the neutrals and their cations at the neutral ground-state structures and the vertical electron detachment energies (VDEs) of $CB_{n-1}(BO)_n^-$ monoanions as the energy differences between the anions and the corresponding neutrals at the anionic ground-state structures have been tabulated in Table 1. All the calculations in this work were carried out using the Gaussian03 program [25].

3 Results and discussion

The lowest-lying positional isomers of $B_n(BO)_n^{2-}$, $CB_{n-1}(BO)_n^-$, and $C_2B_{n-2}(BO)_n$ ($n=5-12$) are shown in Figure 1 with the natural atomic charges indicated for $B_n(BO)_n^{2-}$ dianions in the first column. These structures were obtained by substituting the H atoms in the corresponding $B_nH_n^{2-}$, $CB_{n-1}H_n^-$, and $C_2B_{n-2}H_n$ clusters with boronyl BO groups. As examples, two low-lying positional isomers for $CB_{10}(BO)_{11}^-$ and $C_2B_{10}(BO)_{12}^-$ with the energies relative to their lowest-lying positional isomers are depicted in Figure 2. Figure 3 shows the optimized structures of $B_{11}(BO)_{11}S$ and $B_{11}(BO)_{11}N(BO)$ and Figure 4 shows the variations of the computed magnetic susceptibilities χ (a) and NICS values (b) of the three series versus cluster size n .

As shown in column one of Figure 1, substituting the H atoms in $B_nH_n^{2-}$ with BO radicals produces the ground states of $B_n(BO)_n^{2-}$ dianions which possess exactly the same symmetries as that of the parent boranes $B_nH_n^{2-}$ [1-4], well supporting the BO/H isolobal analogy proposed before [7-15]. Of special interests are the high symmetry $O_h B_6(BO)_6^{2-}$ (2), $D_{4d} B_{10}(BO)_{10}^{2-}$ (6), and $I_h B_{12}(BO)_{12}^{2-}$ (8) which correspond to the highly stable $B_6H_6^{2-}$, $B_{10}H_{10}^{2-}$, and $B_{12}H_{12}^{2-}$ in the $B_nH_n^{2-}$ series, respectively [4]. Concerning the bond parameters of

Table 1 Lowest vibrational frequencies (v_{\min}/cm^{-1}), HOMO energies ($E_{\text{HOMO}}/\text{eV}$), HOMO-LUMO energy gaps ($\Delta E_{\text{gap}}/\text{eV}$), NICS values (NICS/ppm), and magnetic susceptibilities ($\chi/\text{ppm cgs}$) calculated for $B_n(BO)_n^{2-}$, $CB_{n-1}(BO)_n^-$, and $C_2B_{n-2}(BO)_n$ series ($n=5-12$) at the B3LYP/6-311+G(3df) level. The calculated IPs (IP/eV) for $C_2B_{n-2}(BO)_n$ neutrals and VDEs (VDE/eV) for $CB_{n-1}(BO)_n^-$ monoanions have also been tabulated

n	$B_n(BO)_n^{2-}$					$CB_{n-1}(BO)_n^-$					$C_2B_{n-2}(BO)_n$						
	v_{\min}	E_{HOMO}	ΔE_{gap}	NICS	χ	v_{\min}	E_{HOMO}	ΔE_{gap}	NICS	χ	VDE	v_{\min}	E_{HOMO}	ΔE_{gap}	NICS	χ	IP
5	+53	+0.29	4.70	-28.8	-133.5	+58	-4.93	5.64	-21.4	-116.6	6.66	+58	-10.43	6.02	-14.9	-102.3	12.07
6	+60	-1.05	5.81	-22.7	-150.8	+60	-5.69	6.35	-26.3	-140.4	7.31	+55	-10.30	6.16	-27.3	-132.4	11.86
7	+59	-1.70	6.25	-19.6	-171.3	+58	-6.01	6.13	-21.0	-160.2	8.02	+57	-10.71	6.45	-22.4	-151.2	12.18
8	+57	-1.43	4.25	-18.5	-199.2	+56	-6.05	4.51	-18.4	-178.7	7.55	+52	-10.78	4.73	-19.3	-168.1	12.21
9	+60	-2.21	4.31	-23.5	-225.5	+49	-6.63	4.43	-22.3	-208.2	8.05	+52	-10.85	4.43	-22.2	-195.4	12.29
10	+61	-3.21	5.82	-31.1	-262.8	+60	-7.30	5.68	-27.2	-240.2	8.65	+59	-11.28	5.29	-24.8	-220.0	12.60
11	+42	-3.04	4.54	-26.5	-270.8	+45	-7.23	4.44	-24.4	-253.3	8.56	+40	-11.22	4.05	-22.8	-236.7	12.54
12	+66	-4.63	7.07	-24.7	-288.0	+63	-8.07	6.55	-25.1	-275.2	9.35	+59	-11.44	5.93	-26.1	-265.8	12.69

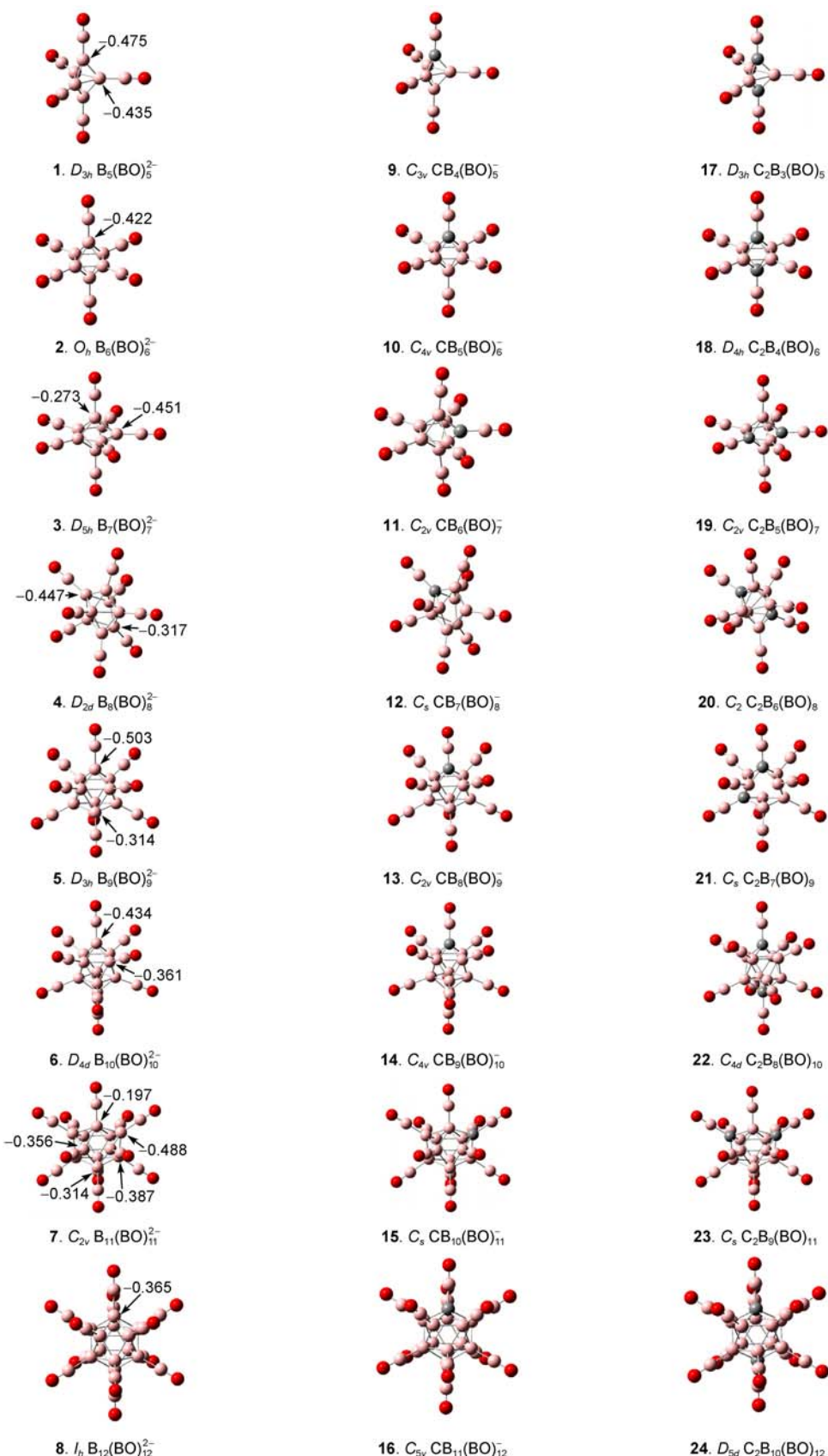


Figure 1 Lowest-lying positional isomers of $B_n(BO)_n^{2-}$, $CB_{n-1}(BO)_n^-$, and $C_2B_{n-2}(BO)_n$ ($n=5-12$) at the DFT level with the natural atomic charges indicated for $B_n(BO)_n^{2-}$ in the first column.

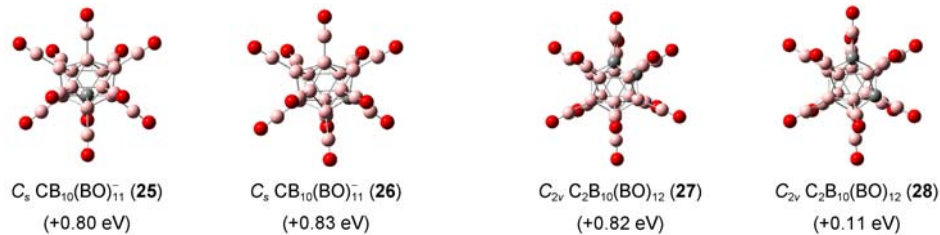


Figure 2 Two positional isomers of $\text{CB}_{10}(\text{BO})_{11}$ (25 and 26) and $\text{C}_2\text{B}_{10}(\text{BO})_{12}$ (27 and 28) with their energies relative to $C_s \text{CB}_{10}(\text{BO})_{11}$ (15) and $D_{5d} \text{C}_2\text{B}_{10}(\text{BO})_{12}$ (24) indicated in parentheses, respectively.

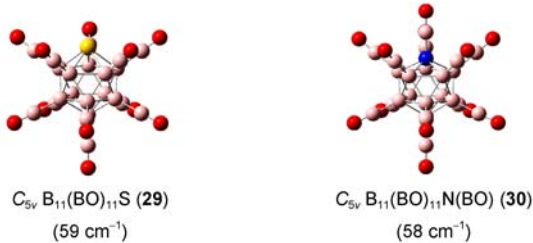


Figure 3 Optimized structures of $C_{5v} \text{B}_{11}(\text{BO})_{11}\text{S}$ (29) and $C_{5v} \text{B}_{11}(\text{BO})_{11}\text{N}(\text{BO})$ (30) with their lowest vibrational frequencies indicated in parentheses.

the $\text{B}_n(\text{BO})_n^{2-}$ series, the skeletal B-B distances on the B_n cages lie in the range 1.655–2.026 Å (close to the corresponding values between 1.614–2.004 Å in $\text{B}_n\text{H}_n^{2-}$) [4], the B-B distances between the B_n cage and the BO terminals fall in the range 1.629–1.661 Å (corresponding to typical B-B single bonds), while the $\text{B}\equiv\text{O}$ distances are slightly elongated to $r_{\text{B}\equiv\text{O}}=1.205\text{--}1.221$ Å from $r_{\text{B}\equiv\text{O}}=1.203$ Å in a free σ -BO radical [13]. Slight $\text{B}\equiv\text{O}$ elongations were also observed in the previously reported $\text{B}(\text{BO})_n$ ($n=2, 3$) [14] and $\text{B}_2(\text{BO})_2^{0/-2-}$ [15].

With one skeleton B substituted by a C atom at different

vertexes of a $\text{B}_n(\text{BO})_n^{2-}$ cage, several positional isomers are produced for each $\text{CB}_{n-1}(\text{BO})_n^-$ species. Similar to the situation in monocarboranes $\text{CB}_{n-1}\text{H}_n^-$ [5, 6], the highly electronegative C atoms occupy the vertexes with the highest electronic densities [4]. Applying this “selection” rule to $\text{B}_n(\text{BO})_n^{2-}$ dianions in column one according to their atomic charge distributions shown in Figure 1 produces the lowest-lying structures of $\text{CB}_{n-1}(\text{BO})_n^-$ monoanions in column two. All the other positional isomers prove to be less stable. As examples, two low-lying positional isomers of $\text{CB}_{10}(\text{BO})_{11}$ (C_s 25 and C_s 26) are shown in Figure 2 which both proved to be clearly less stable than $C_s \text{CB}_{10}(\text{BO})_{11}$ (15).

With one more skeleton B in $\text{CB}_{n-1}(\text{BO})_n^-$ in column two substituted with a second C atom, the $\text{C}_2\text{B}_{n-2}(\text{BO})_n$ neutrals in column three are produced, very similar to the situation in dicarboranes $\text{C}_2\text{B}_{n-2}\text{H}_n$ [1–4]. With two C atoms present in $\text{C}_2\text{B}_{n-2}(\text{BO})_n$, the second C prefers a nonadjacent site to form more B-C interactions which are favored in energy over C-C interactions [4]. As examples, Figure 2 depicts two low-lying positional isomers for neutral $\text{C}_2\text{B}_{10}(\text{BO})_{12}$ (C_{2v} 27 and C_{2v} 28). Both of these isomers proved to lie higher in energy relative to the lowest-lying $D_{5d} \text{C}_2\text{B}_{10}(\text{BO})_{12}$ (24).

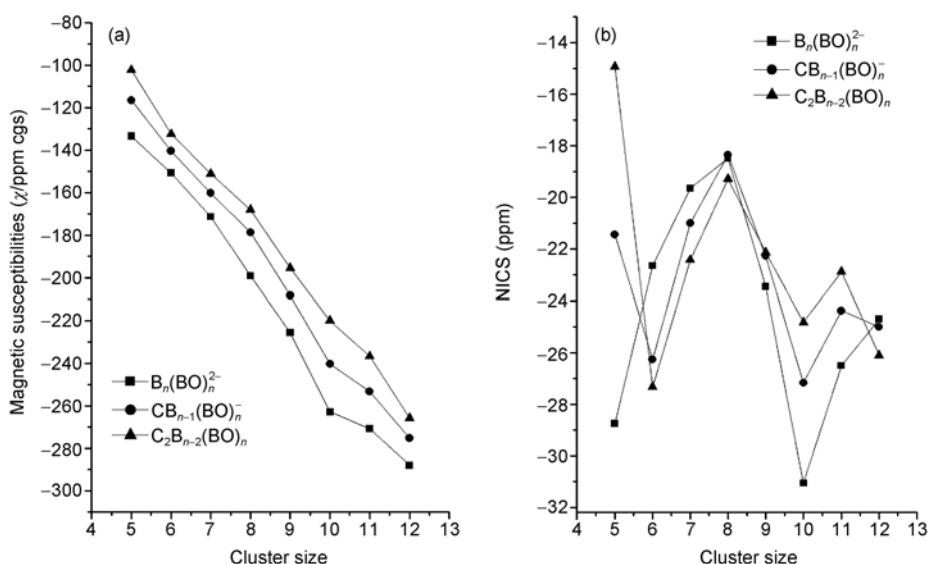


Figure 4 Calculated magnetic susceptibilities x (a) and NICS values (b) versus cluster sizes n for $\text{B}_n(\text{BO})_n^{2-}$, $\text{CB}_{n-1}(\text{BO})_n^-$, and $\text{C}_2\text{B}_{n-2}(\text{BO})_n$ series.

The possibilities to substitute a skeletal B atom in I_h $B_{12}(BO)_{12}^{2-}$ with a N or an S atom have also been investigated. As shown in Figure 3, both the neutral C_{5v} $B_{11}(BO)_{11}S$ (**29**) and C_{5v} $B_{11}(BO)_{11}N(BO)$ (**30**) are true minima on the potential surfaces of the corresponding systems. N and S atoms on the five-fold molecular axes match the 12-membered cage both electronically and geometrically. However, an O atom proved to be too small in size to form a stable cage-like C_{5v} $B_{11}(BO)_{11}O$.

The calculated magnetic susceptibilities possess increasingly negative values between $\chi = -102$ and -288 ppm cgs for all the three $B_n(BO)_n^{2-}$, $CB_{n-1}(BO)_n^-$, and $C_2B_{n-2}(BO)_n$ ($n = 5-12$) series (see Table 1 and Figure 4(a)), very similar to the situation in the 3D aromatic $B_nH_n^{2-}$, $CB_{n-1}H_n^-$, and $C_2B_{n-2}H_n$ [4]. These cage-like boron boronyls also possess negative NICS values between -14.9 and -31.1 ppm in all the three series, with the 6, 10, and 12 vertex structures possessing the most negative NICS values at their cage centers and therefore being most 3D aromatic (see Figure 4(b)) (except for $B_6(BO)_6^{2-}$ and $B_{12}(BO)_{12}^{2-}$ dianions for which the negative NICS values do not follow the stabilities of the clusters possibly due to the high charges the dianions carry). Molecular orbital delocalizations and 3D ring current effects exist in these cage-like structures, well paralleling the corresponding boranes, monocarboranes, and dicarboranes [4, 5].

As shown in Table 1, $C_2B_{n-2}(BO)_n$ neutrals ($n = 5-12$) possess huge negative HOMO eigenvalues ($E_{\text{HOMO}} = -10.3$ – -11.5 eV) and wide HOMO-LUMO energy gaps ($\Delta E_{\text{gap}} = 4.05$ – 6.45 eV), showing their high electronic stabilities. Consequently, these neutrals have considerably high ionization potentials (IPs) in the range $\text{IP} = 12.0$ – 12.7 eV. The prototypical D_{5d} $C_2B_{10}(BO)_{12}$ has the lowest HOMO energy (-11.44 eV) and highest IP value (12.69 eV) in the $C_2B_{n-2}(BO)_n$ series. These values are even higher than $\text{HOMO} = -8.85$ eV and $\text{IP} = 10.88$ eV obtained for D_{5d} $C_2B_{10}H_{12}$ at the same theoretical level. $CB_{n-1}(BO)_n^-$ monoanions possess the HOMO energies between $E_{\text{HOMO}} = -4.93$ eV and -8.07 eV and the vertical electron detachment energies (VDEs) in the range 6.6–9.4 eV. Again, C_{5v} $CB_{11}(BO)_{12}^-$ has the lowest HOMO energy and the highest VDE value (See Table 1) in the $CB_{n-1}(BO)_n^-$ series. $B_n(BO)_n^{2-}$ dianions have much less negative HOMO energies ($E_{\text{HOMO}} = +0.29$ – -4.63 eV) than both $C_2B_{n-2}(BO)_n$ and $CB_{n-1}(BO)_n^-$ (with the smallest cage-like D_{3h} $B_5(BO)_5^{2-}$ even possessing a positive HOMO energy ($E_{\text{HOMO}} = +0.29$ eV)). The $B_n(BO)_n^{2-}$ closo-borane dianions carry the highest negative charges and have the least negative HOMO energies in the three series. However, these dianions are expected to be effectively stabilized when counterions (like Li^+) are incorporated into the systems [12, 15]. The huge calculated HOMO-LUMO energy gaps in Table 1 also reveal an interesting alternating pattern for each series: ΔE_{gap} values reach their maxima at

$n = 6, 10$, and 12 for both $B_n(BO)_n^{2-}$ and $C_2B_{n-2}(BO)_n$ series and $n = 7, 10$, and 12 for $CB_{n-1}(BO)_n^-$, well in line with the high electronic stabilities of the high symmetry deltahedral clusters.

The calculated BO stretching vibrational frequencies of I_h $B_{12}(BO)_{12}^{2-}$ ($\nu_{\text{BO}} = 2003$ cm $^{-1}$), C_{5v} $CB_{11}(BO)_{12}^-$ ($\nu_{\text{BO}} = 2033$ cm $^{-1}$), and D_{5d} $C_2B_{10}(BO)_{12}$ ($\nu_{\text{BO}} = 2055$ cm $^{-1}$) lie slightly higher than the measured $\text{B} \equiv \text{O}$ characteristic vibrational frequency in free BO^- ($\nu_{\text{BO}} = 1935$ cm $^{-1}$) [13] and crystal $[(\text{Cy}_3\text{P})_2\text{BrPt}(\text{BO})]$ ($\nu_{\text{BO}} = 1979$ and 1853 cm $^{-1}$) [19], indicating that triplet $\text{B} \equiv \text{O}$ bonds have been well maintained in these boron oxide clusters. The $\text{B} \equiv \text{O}$ vibrational frequency at about 2000 cm $^{-1}$ in the three series can be utilized to characterize the BO terminals in future IR measurements.

4 Summary

$B_n(BO)_n^{2-}$, $CB_{n-1}(BO)_n^-$, and $C_2B_{n-2}(BO)_n$ ($n = 5-12$) clusters have been predicted at the DFT level to be the boronyl analogues of the *closo*-species $B_nH_n^{2-}$, $CB_{n-1}H_n^-$, and $C_2B_{n-2}H_n$, well supporting the BO/H isolobal analogy in small boron-rich boron oxide clusters. These cage-like structures with both negative NICS and χ values prove to be 3D aromatic. $C_2B_{n-2}(BO)_n$ neutrals possess considerably high IPs (above 12.0 eV) and $CB_{n-1}H_n^-$ monoanions have very high VDEs (above 6.6 eV). The characteristic $\text{B} \equiv \text{O}$ stretching vibrational frequencies at about 2000 cm $^{-1}$ can be used to identify these clusters in future IR measurements. We anticipate that, similar to its CN counterpart, a BO group may be incorporated in a wide range of inorganic and organic compounds in the near future to open the area of boronyl chemistry [6–15, 19]. Combined experimental and theoretical investigations in this direction are currently underway in our group.

This work was jointly supported by the National Natural Science Foundation of China (20873117) and the Shanxi Natural Science Foundation (2010011012-3).

- 1 Cotton FA, Wilkinson G, Murillo CA, and Bochmann M. *Advanced Inorganic Chemistry*, 6th ed. New York: Wiley, 1999
- 2 Onak T. Polyhedral carbaboranes. In: Abel EW, Stone FG, Wilkinson G, Eds. *Comprehensive Organometallic Chemistry II*. Oxford: Pergamon Press, 1995. Vol. 6, Chapter 6
- 3 Mings DMP, Wales DJ. *Introduction to Cluster Chemistry*. Englewood Cliffs: Prentice Hall 1990
- 4 Schleyer PvR, Najafian K. Stability and three-dimensional aromaticity of closo-monocarborane anions, $CB_{n-1}H_n^-$, and closo-dicarboranes, $C_2B_{n-2}H_n$. *Inorg Chem*, 1998, 37: 3454–3470
- 5 McKee ML, Wang ZX, Schleyer PvR. *Ab initio* study of the hypercloso boron hydrides B_nH_n and $B_nH_n^-$. Exceptional stability of neutral $B_{13}H_{13}$. *J Am Chem Soc*, 2000, 122: 4781–4795
- 6 Doyle J. High-molecular-weight boron oxides in the gas phase. *J Am Chem Soc*, 1988, 110: 4120–4126
- 7 Li SD, Miao CQ, Guo JC, Ren GM. Carbon boronyls: Species with higher viable possibility than boron carbonyls at the density func-

- tional theory. *J Comput Chem*, 2005, 26: 799–802
- 8 Ren GM, Li SD, Miao CQ. Sandwich-type transition metal complexes $[(\text{CBO})_n]_2\text{M}$ with carbon boronyl ligands (CBO_n) ($n=4\text{--}6$). *J Mol Struct: THEOCHEM*, 2006, 770: 193–197
- 9 Li SD, Guo JC, Ren GM. Density functional theory investigations on boronyl-substituted ethylenes $\text{C}_2\text{H}_{4-m}(\text{BO})_m$ ($m=1\text{--}4$) and acetylenes $\text{C}_2\text{H}_{2-m}(\text{BO})_m$ ($m=1, 2$). *J Mol Struct: THEOCHEM*, 2007, 821: 153–159
- 10 Yao WZ, Guo JC, Lu HG, Li SD. $T_d \text{B}(\text{BO})_4^-$: A tetrahedral boron oxide cluster analogous to boron hydride $T_d \text{BH}_4^-$. *J Phys Chem A*, 2009, 113: 2561–2564
- 11 Guo QL, Guo JC, Li SD. Geometries, electronic structures, and electron detachment energies of small boron sulfide anions: A density functional theory investigation. *Chin J Struct Chem*, 2008, 6: 651–658
- 12 Yao WZ, Guo JC, Lu HG, Li SD. $D_{\infty h} \text{B}_2(\text{BS})_2^{-2-}$ and $T_d \text{B}(\text{BS})_4^-$: Boron sulfide clusters containing BB multiple bonds and B⁻ tetrahedral centers. *Int J Quantum Chem*, 2010, 110: 2689–2696
- 13 Zhai HJ, Wang LM, Li SD, Wang LS. vibrationally resolved photo-electron spectroscopy of BO^- and BO_3^- : A joint experimental and theoretical study. *J Phys Chem A*, 2007, 111: 1030–1035
- 14 Zhai HJ, Li SD, Wang LS. Boronyls as key structural units in boron oxide clusters: $\text{B}(\text{BO})_2^-$ and $\text{B}(\text{BO})_3^-$. *J Am Chem Soc*, 2007, 129: 9254–9255
- 15 Li SD, Zhai HJ, Wang LS. $\text{B}_2(\text{BO})_2^{2-}$ –diboronyl diborene: A linear molecule with a triple boron–boron bond. *J Am Chem Soc*, 2008, 130: 2573–2579
- 16 Drummond ML, Meunier V, Sumpter BG. Structure and stability of small boron and boron oxides clusters. *J Phys Chem A*, 2007, 111: 6539–6551
- 17 Nguyen MT, Matus MH, Ngan VT, Grant DJ, Dixon DA. Thermochemistry and electronic structure of small boron and boron oxides clusters and their anions. *J Phys Chem A*, 2009, 113: 4895–4909
- 18 Tai TB, Nguyen MT, Dixon DA. Thermochemical properties and electronic structure of boron oxides B_nO_m ($n=5\text{--}10$, $m=1\text{--}20$) and their anions. *J Phys Chem A*, 2010, 114: 2893–2912
- 19 Braunschweig H, Radacki K, Schneider A. Oxboryl complexes: Boron–oxygen triple bonds stabilized in the coordination sphere of platinum. *Science*, 2010, 328: 345–347
- 20 Beck AD. Density functional thermochemistry. III. The role of exact exchange. *J Chem Phys*, 1993, 98: 5648–5659
- 21 Lee C, Yang W, Parr RG. Development of the Colle–Salvetti correlation energy formula into a functional of the electron density. *Phys Rev B*, 1988, 37: 785–791
- 22 Schleyer PvR, Maerker C, Dransfeld A, Jiao H, van Eikema Hommes NJR. Nucleus-independent chemical shifts: A simple and efficient aromaticity probe. *J Am Chem Soc*, 1996, 118: 6317–6318
- 23 Bader RFW, Keith TA. Properties of atoms in molecules: Magnetic susceptibilities. *J Chem Phys*, 1993, 99: 3683–3693
- 24 Keith TA, Bader RFW. Calculation of magnetic response properties using atoms in molecules. *Chem Phys Lett*, 1992, 194: 1–8
- 25 Frisch MJ, Trucks GW, Schlegel HB, Scuseria GE, Robb MA, Cheeseman JR, Montgomery JA Jr, Vreven T, Kudin KN, Burant JC, Millam JM, Iyengar SS, Tomasi J, Barone V, Mennucci B, Cossi M, Scalmani G, Rega N, Petersson GA, Nakatsuji H, Hada M, Ehara M, Toyota K, Fukuda R, Hasegawa J, Ishida M, Nakajima T, Honda Y, Kitao O, Nakai H, Klene M, Li X, Knox JE, Hratchian HP, Cross JB, Adamo C, Jaramillo J, Gomperts R, Stratmann RE, Yazyev O, Austin AJ, Cammi R, Pomelli C, Ochterski JW, Ayala PY, Morokuma K, Voth GA, Salvador P, Dannenberg JJ, Zakrzewski VG, Dapprich S, Daniels AD, Strain MC, Farkas O, Malick DK, Rabuck AD, Raghavachari K, Foresman JB, Ortiz JV, Cui Q, Baboul AG, Clifford S, Cioslowski J, Stefanov BB, Liu G, Liashenko A, Piskorz P, Komaromi I, Martin RL, Fox DJ, Keith T, Al-Laham MA, Peng CY, Nanayakkara A, Challacombe M, Gill PMW, Johnson B, Chen W, Wong MW, Gonzalez C, Pople JA. Gaussian 03, Revision A.1. Pittsburgh: Gaussian, Inc., 2003